Photo-thermal nonlinearity enhancement in dye-doped liquid crystals by polymer doping

Liquid Crystals

ISSN: 0267-8292 (Print) 1366-5855 (Online) Journal homepage: www.tandfonline.com/journals/tlct20

Photo-thermal nonlinearity enhancement in dye-doped liquid crystals by polymer doping

Federico Massarelli, Diederik Sybolt Wiersma, Francesco Riboli & Sara Nocentini

To cite this article: Federico Massarelli, Diederik Sybolt Wiersma, Francesco Riboli & Sara Nocentini (28 Jul 2025): Photo-thermal nonlinearity enhancement in dye-doped liquid crystals by polymer doping, Liquid Crystals, DOI: 10.1080/02678292.2025.2531107

To link to this article: https://doi.org/10.1080/02678292.2025.2531107

Published online: 28 Jul 2025.

LIQUID CRYSTALS
https://doi.org/10.1080/02678292.2025.2531107

Photo-thermal nonlinearity enhancement in dye-doped liquid crystals by polymer doping

Federico Massarelli[a], Diederik Sybolt Wiersma[a,b,c], Francesco Riboli[a,d] and Sara Nocentini[a,b]

[a]European Laboratory for Non-Linear Spectroscopy (LENS), University of Florence, Sesto Fiorentino, Florence, Italy; [b]Division of Metrology of Innovative Materials and Life Sciences, Istituto Nazionale di Ricerca Metrologica (INRiM), Turin, Italy; [c]Department of Physics and Astronomy, University of Florence, Sesto Fiorentino, Florence, Italy; [d]Consiglio Nazionale delle Ricerche – Istituto Nazionale di Ottica (CNR-INO), Sesto Fiorentino, Florence, Italy

ABSTRACT

Nonlinear photonic materials play an important role in the development of advanced optical and photonic technologies. Third-order optical nonlinearity is at the basis of effects like self-modulation and threshold phenomena and can be used for fast tuning and optical switching. Dye-doped nematic liquid crystals are characterised by outstanding values of the nonlinear refractive index. However, in resonance conditions, they suffer from energy loss due to absorption. In this work, we demonstrate large photo-thermal nonlinearity in dye-doped linear Polymer-Stabilized Liquid Crystals (PSLCs) and show how to tune their nonlinear refractive index by tailoring the chemical formulation. Dye-doped PSLC are probed with pre-resonant light at very low power and are characterised by the Z-scan technique. This approach, which strongly limits losses, proves to preserve the nonlinear response despite the pre-resonance illumination. Moreover, the linear polymeric structure turns out to enhance the third-order optical nonlinearity and make its response faster. We thus obtain a controllable nonlinear refractive index that reaches values of around 10^{-5} $cm^2 \cdot W^{-1}$ with pre-resonant light in a characteristic time of about 1.5 ms, offering low energy loss, remarkable features in terms of nonlinearity and time response that can strongly impact integrated photonics, cryptography and optical computing applications.

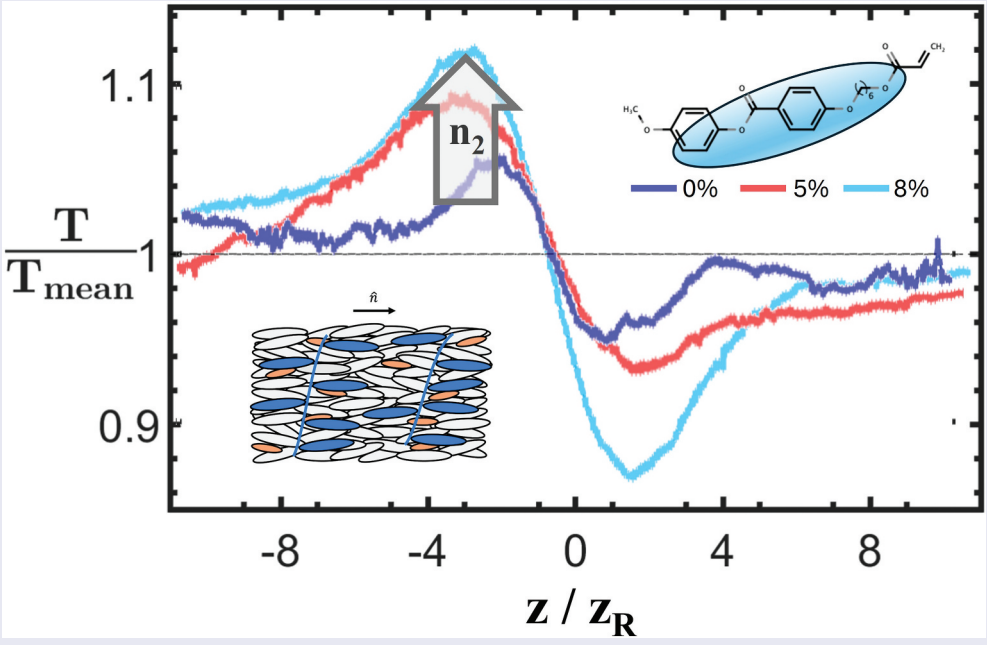

ARTICLE HISTORY
Received 14 February 2025
Accepted 3 July 2025

KEYWORDS
Third order nonlinearity; Z-scan setup; dye-doped liquid crystals; polymer-stabilized liquid crystals; polymer concentration

CONTACT Sara Nocentini nocentini@lens.unifi.it; s.nocentini@inrim.it

1. Introduction

Low-power nonlinear optical responses represent a breakthrough for the future realisation of new cryptographic and photonic functions, as they could enable operations that would otherwise be impossible in the linear regime and can be applied to very large scale integration. At present, they can be achieved only at very high intensities in suitable media, leading to nonlinear effects that include self-focusing [1], solitons [2] and high-harmonic generation [3]. Such nonlinearities are employed in several fields and became more and more relevant to advance photonic platforms in integrated photonics for all-optical switches [4,5], in cryptography to improve the security of a new generation of key generators, the so-called Physical Unclonable Functions (PUFs) [6,7], and in optical computing to produce nonlinear activation functions [8,9]. Among all-optical nonlinear phenomena, the optical Kerr and Kerr-like effects induce a refractive index change that depends on the intensity of the optical radiation. In this way, the modulation of the signal is induced by the propagating light itself, without the need for external fields, thus making this effect particularly interesting and easy to integrate for the above-mentioned applications. A wide variety of nonlinear materials have been studied for integrated photonics including semiconductors, glasses, 2D materials, and polymers, whose nonlinear refractive indexes range from 10^{-16} cm^2 W^{-1} to 10^{-10} cm^2 W^{-1} [10]. Semiconductor and polymeric materials offer good integrability, but require very high intensities (of the order of magnitude of 10^{10} W cm^{-2} that can be achieved by high-power pulsed laser) to induce a considerable variation in the refractive index [11]. To strongly reduce power consumption and make these functions scalable on a large scale, a nonlinear response that can be activated by low-power continuous-wave lasers should be found. The materials that provide the largest nonlinearity but at the slowest response time are nematic liquid crystals (LCs) [12], whose nonlinear coefficient ranges from 10^{-5} $cm^2 \cdot W^{-1}$ to 10^{-3} $cm^2 \cdot W^{-1}$ [13,14] for transparent nematic liquid crystals and dye-doped nematic liquid crystals, respectively. This type of large nonlinearity peculiar to LCs is based on collective reorientational phenomena that are characterized by large and relatively slow nonlinearities (with a typical response time $\tau > \mu s$) besides molecular electronic nonlinearities common to all the materials. Among the collective nonlinearities in LC there are a few mechanisms that enhance the nonlinear response depending on the formulation and the type of laser excitation. The strong optical nonlinearity peculiar to nematic liquid crystals is often called 'Giant optical nonlinearity' because of their high values of nonlinear refractive index and it is mainly associated with an electromagnetic torque on the LC molecules (that can be enhanced in presence of a dye). On the other hand, the molecular reorientation can also be driven by a thermo-optical effect that is mainly studied in resonant conditions. Liquid crystal nonlinearity has been deeply studied since the '80s with different formulations, evaluating different contributions to nonlinearity [13,14]. However, the majority of the studies are focused on liquid formulations and a few examples are reported for polymer-stabilised liquid crystals (PSLC). PSLC are composed of linear polymeric chains or crosslinked polymeric networks in which the liquid crystalline molecules are immersed [15]. Their study for nonlinear devices is limited to a few works in which it has been reported that dispersing a small amount of polymer, (around 10 percent in weight) in a dye-doped liquid crystal, thus making a so-called dye-doped Polymer-Stabilized Liquid Crystal (dye-doped PSLC) [16], leads to an increase in the nonlinear response in resonant conditions [17–19]. In the latter, the nonlinearity of dye-doped PSLCs results from optical and thermal liquid crystal collective reorientation induced by the dye absorption that however generates large optical losses, which are detrimental for optical applications [20]. On the other hand, a systematic study of the nonlinear response of dye-doped PSLCs with non-resonant light and its underlying mechanism is still missing. To fill this gap, we herein study dye-doped polymer-stabilized nematic liquid crystals with different linear polymer and dye concentrations to optimize the nonlinear response and highlight the role of the stabilizing polymer. In this way, we achieve large photo-thermal nonlinearity with a sixth-fold optimisation in the polymer stabilised formulation and a faster nonlinearity dynamics with respect to the pure liquid crystal in pre-resonant condition. These promising values in low-loss nonlinear materials open to a new paradigm of nonlinear functions in integrated photonics, cryptography and optical computing.

2. Methodology

2.1. PSLC formulations

We study liquid-crystal-based photonic materials and their photo-thermal nonlinearity, focusing on the nonlinearity of formulations with dye-doped Liquid Crystals (LCs) and dye-doped linear Polymer-Stabilized Liquid Crystals (PSLCs).

The analysis of the nonlinearity is performed by tailoring their formulations. More in detail, we vary the type of dye molecule and/or the polymer concentration, which ranges from 0% to 30%.

Dye-doped PSLCs are made of four different components: liquid crystals, dye molecules, a polymeric structure, and a photo-initiator.

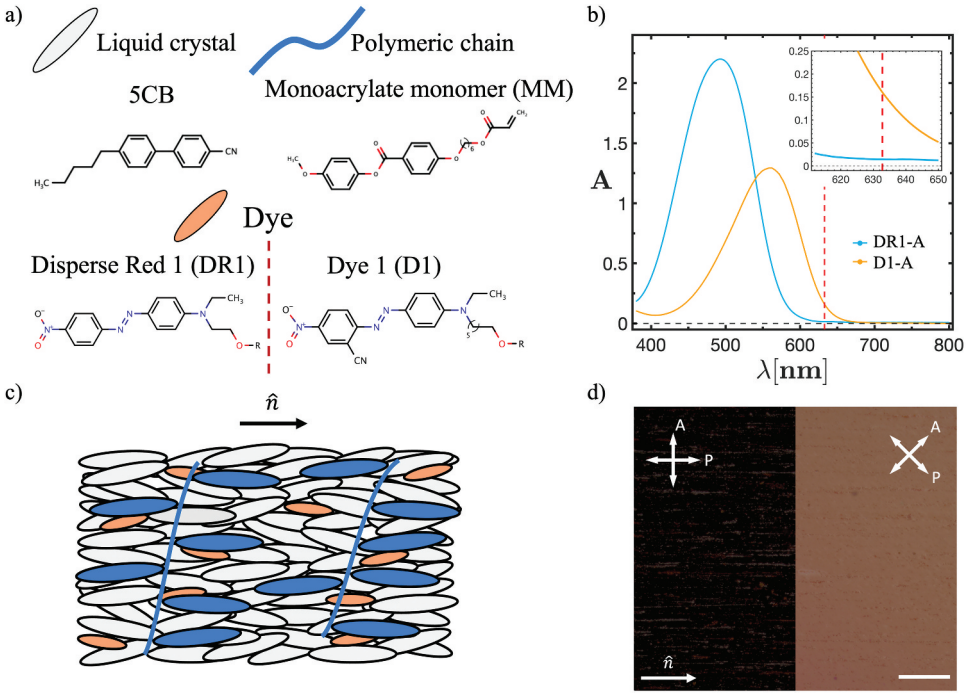

Figure 1. (Colour online) Dye-doped polymer-stabilized liquid crystals. (a) Structural formulas of the used molecules. The formulas relating to disperse red 1 and dye 1 are presented with a functional group -R, which is a hydrogen atom or an acrylate group depending on the non-acrylate or acrylate nature of the molecule, respectively. (b) Absorption spectra of LCs doped with 1% dye for a polarization parallel to the LC alignment (director). The dotted red line denotes the He-Ne laser wavelength, 633 nm, of the He-Ne laser used in the optical measurements. The inset at the top right reports a zoom of the spectra in the wavelength range between 612 nm and 650 nm, while the legend refers to the kind of dye in the dye-doped liquid crystal under examination, where the suffix "-A" in the names of the dyes indicates their acrylate nature. (c) Schematic representation of a dye-doped polymer-stabilized liquid crystal. Its molecular alignment is indicated with the LC director denoted by the versor $\hat{n}$ over the drawing, where the gray and orange molecules correspond to liquid crystals and dyes, respectively, while the blue curves and molecules refer to the polymeric chains. (d) Combination of polarized optical microscope images relating to an illustrative dye- doped PSLC with 1% dye DR1-A and 15% monoacrylate monomer MM. Besides the LC director $\hat{n}$, also the orientation of fast axis of the polarizer (P) and analyzer (A) filters are indicated. The scale bar is 100 μm.

As liquid-crystalline mesogen, the nematic liquid crystal 4-Cyano-4'-pentylbiphenyl, which is commercially called 5CB (SYNTHON Chemicals), is chosen, and its structural formula is reported in Figure 1(a).

Concerning the dye molecule, two different azobenzenes are used: Disperse Red 1 (DR1) and Dye 1 (D1). Their structural formulas are shown in Figure 1(a). Disperse Red 1 is a commercial molecule and is purchased by Sigma-Aldrich, while Dye 1 is synthesised by our research group [21–23]. Disperse Red 1 and Dye 1 are tested in two forms, with or without an acrylate group. In the case of the acrylate terminated dye, hereafter they are named as Disperse Red 1 acrylate (DR1-A) and Dye 1 acrylate (D1-A), otherwise Disperse Red 1 non-acrylate (DR1-NA) and Dye 1 non-acrylate (D1-NA). These dyes are chosen because they are characterised by a low but not negligible absorption at 633 nm, the wavelength of the He-Ne laser used in the experiments, as can be seen from the absorption spectra of Figure 1(b). It shows the spectra of the dye-doped LC for a probing light with a polarisation that is parallel to the LC alignment or to the director. The inset in Figure 1(b) zooms into their absorbance in the wavelength range between 612 nm and 650 nm, highlighting the small but not negligible absorption at 633 nm for the dye DR1-A, that is almost one order of magnitude smaller than of D1-A.

The polymeric structure is formed starting from monoacrylate monomers. The Monoacrylate Monomer (MM) is a commercial molecule (CAS 130,953–14–9, Sigma-Aldrich), that creates linear polymeric chains. The structural formula of the monomer is presented in Figure 1(a), while a picture schematising the involved molecules and their alignment is shown in Figure 1(c), where the versor $\hat{n}$ denotes the direction of the liquid-crystalline orientational order, the so-called LC director.

About the photo-initiator, the UV photo-initiator Irgacure 369 (IN) is selected. In the PSLC formulations, the concentration in weight of the initiator is fixed at 1%. From now onwards all concentrations are meant to be expressed in weight.

The polymerisation of a PSLC is performed by exposing the monomeric mixture to a UV LED lamp (Thorlabs M385LP1-C) with a peak wavelength of 385 nm and a power of around 660 mW for twenty minutes. The temperature is maintained at 22°C for the first ten minutes, so that the polymerisation is almost completed with the LC sample in the nematic phase, while the temperature is increased at 40°C for the second ten minutes to assure a complete polymerisation of the sample. Indeed, the liquid crystal 5CB is in the nematic phase at room temperature, being in the crystalline phase under approximately 11°C and in the isotropic phase above about 34°C, as verified by differential scanning calorimetry measurements [24]. As for the LC alignment, we focus on homogeneous planar alignment, which is obtained by LC molecule interaction with properly treated glass coverslips. They are spin-coated with an aqueous solution of 5% PolyVinyl Alcohol (PVA, CAS 9002–89–5, Sigma-Aldrich), and rubbed with a velvet cloth in the direction of alignment before creating an LC cell two glass coverslips and infiltrating it with the LC mixture.

The LC alignment is verified by Polarized Optical Microscopy (POM), and along this study, every sample is characterised at the Polarized Optical Microscope (POM) (Zeiss Axio Observer A1), before and after the polymerisation process (if present), in order to qualitatively assess the degree of molecular alignment and its homogeneity. When the LC director is parallel to one of the two crossed polarisers of the POM, the transmission through the sample is almost extinguished and the image appears homogeneous and dark, while, when the LC director is at 45° to the directions of the two polarisers, the homogeneously aligned samples allows for a light polarisation rotation that makes the image homogeneous and luminous.

An illustrative POM image for a dye-doped PSLC with 1% dye DR1-A and 15% monoacrylate monomer MM, is shown in Figure 1(d), where it can be seen that a few defects only marginally affect the homogeneous planar alignment. It is chosen among the various types of alignment because it allows a good alignment [25], as seen in Figure 1(d), without considerable manufacturing efforts and because of its interesting interaction with linearly polarised light.

The thickness of a sample is fixed by silica microspheres (Thermo Fisher Scientific) with diameters of 20 μm, which separate the glass coverslips that make up a cell.

2.2. Z-scan set-up

Among the third order nonlinear phenomena, the Kerr-like effect refers to the dependence of the refractive index n on the light intensity I : $n = n_0 + n_2 \cdot I$ (Equation 1) where n_2 is the nonlinear refractive index.

A standard way to measure the nonlinear refractive index is the so-called Z-scan technique [12], which retrieves the nonlinear coefficient through a measure of self-focusing or self-defocusing effect [1]. The characterisation of optical nonlinearity is performed using a conventional Z-scan set-up. Figure 2(a,b) shows the picture of the experimental apparatus. More in detail, the intensity of a focused laser beam impinging on a sample is varied through a scan of the sample along the optical axis, defined as z-axis, and the transmitted light passing through an iris is collected for each sample position along the z-axis. Changes in the refractive index due to nonlinear optical effects in the sample are detected as characteristic intensity variations in the transmitted signal as a function of the sample position because of the effects of self-focusing and self-defocusing. With this technique both the sign and the absolute value of the nonlinear refractive index can be deduced from the transmission curve: if the iris is partially closed, in the so-called closed-aperture configuration, the measured quantity is the nonlinear refractive index, while, if the iris is left totally open, in the so-called open-aperture configuration, the measured quantity is the nonlinear absorption coefficient [26,27]. Since the samples considered in this article do not show detectable nonlinear absorption, all reported measurements refer to the experimental configuration with the iris partially closed. Focusing on the configuration with the iris partially closed from now on, the sign of the nonlinear refractive index can be determined by looking at the position of the peak and the valley of the transmission curve in the Z-scan graph. An illustrative measurement of PSLC nonlinearity is reported in Figure 2(b) for a sample with negative n_2: indeed, if the valley and the peak are at negative and positive z-values, respectively, the sign of the nonlinear refractive index is positive, while it is negative if their positions are exchanged. The absolute value of the nonlinear refractive index is calculated from the Z-scan curve by taking advantage of the direct proportionality between the absolute value of the nonlinear refractive index n_2 and the peak-to-valley difference ΔT extracted from the curve [12].

In addition, the nature of the nonlinear optical response of a sample, reorientational and/or thermal, can be established on the basis of the peak-to-valley distance along the z-axis in the Z-scan graph, Δz_{p-v}. Indeed, values of $\Delta z_{p-v} = 1.72\, z_R$ and $\Delta z_{p-v} = 3.46\, z_R$, where z_R is the Rayleigh length of the focused beam, are characteristics of the reorientational and thermal effects, respectively [28,29].

The laser source of the Z-scan set-up is a He-Ne laser (633 nm, Thorlabs HNL050L). The laser beam passes

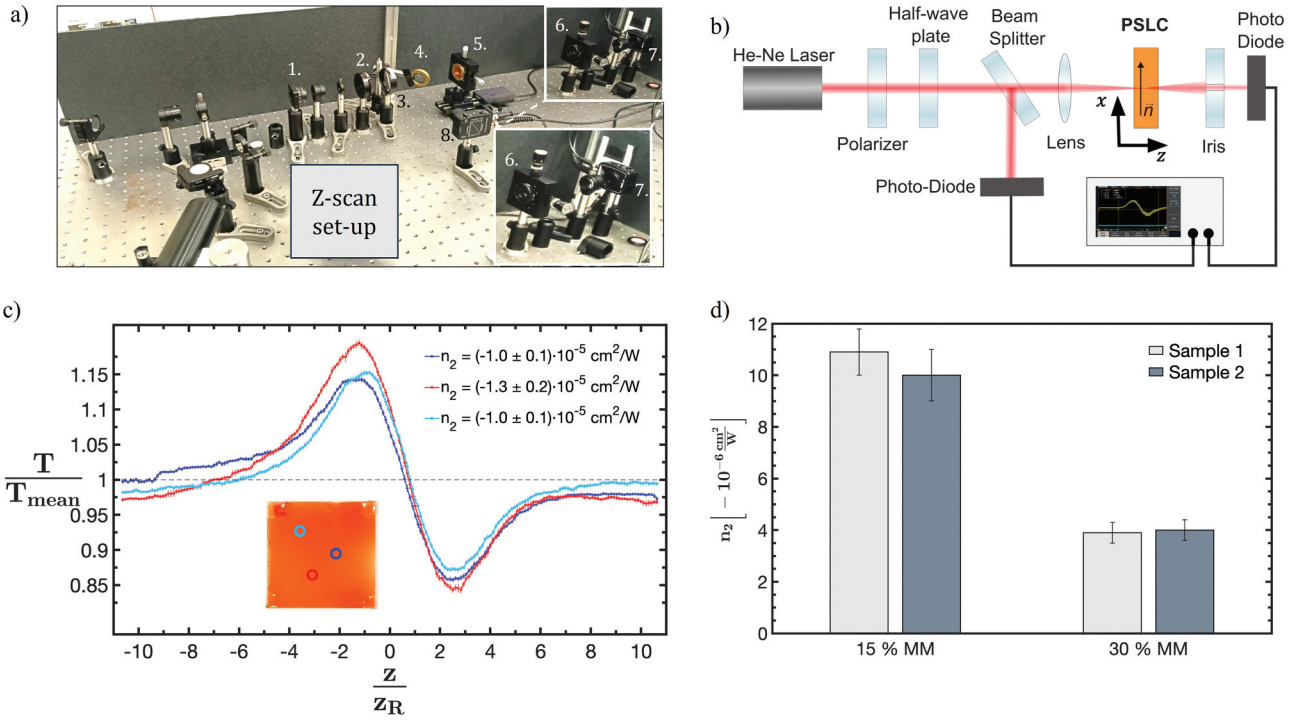

Figure 2. (Colour online) Z-scan set-up and illustrative measurements. (a) Photograph of the Z-scan set-up. Some optical elements are signposted by numbers: a polarizer filter (1), a half-wave plate (2), a converging lens (3), a beam splitter (4), a sample (5), an iris (6) and detectors (7 and 8). The inset zooms on the iris and the detector. (b) Schematics of the main optical elements of the Z-scan setup. (c) Illustrative Z-scan curves for three different points on a dye-doped PSLC with 1% dye DR1-A and 15% monoacrylate monomer MM. The transmittance is normalized by its average value T_{mean}, while the position along the z-axis is normalized by the Rayleigh length z_R of the focused beam. The inset box shows a photo of the measured sample, wherein the circles indicate the measured areas of the sample for which the z-scan curves are reported in the graph with the same colors. (d) Reproducibility of the Z-scan measurements between different samples with the same chemical formulation for 15% and 30% monomer concentrations. The mean value for each sample is calculated over three measured points on the sample and the error bar corresponds to a weighted sum of the standard deviations.

through a polariser filter and a half-wave plate before being focused by a converging lens with a focal length of 150 mm on the sample, which is moved by a translation stage (Thorlabs Z812B) in an interval of 20 mm along the z-axis with a speed equal to 0.20 mm·s^{-1} during the scan. The laser spot diameter ranges from about 14 μm when the sample is at the focus, to around 167 μm when the sample is at 10 mm away from the focus. As the Rayleigh length of the Gaussian beam is approximately 940 µm and the sample thickness is 20 μm, the sample is thin enough and scanned over a large distance (z-axis translation from −10 mm to 10 mm) to be probed by laser intensities that vary considerably. The light power at the sample is around 2.40 mW, while the intensity at the focus is about $3.8 \cdot 10^2$ W·cm^{-2}. We monitor any laser intensity fluctuations by a reference beam measured before passing through the sample. The two parameters of illumination that can be adjusted are the intensity of the radiation, which is controlled by neutral density filters, and its polarization, which is varied by means of a half-wave plate. The laser power and the photodiodes used in the experimental set-up allow us to detect nonlinear refractive indexes whose order of magnitude is larger than 10^{-7} cm^2·W^{-1}.

First, we test the nonlinearity of the pure LC 5CB with homogeneous planar alignment, but since its nonlinear coefficient is under our detection limit, we cannot measure it. Therefore, we exploit the dye molecules to enhance and observe the nonlinear response in LC formulation [13,14].

An illustrative example of Z-scan transmission curves is shown in Figure 2(c). These curves refer to three different points on a dye-doped PSLC with 1% dye DR1-A and 15% monoacrylate monomer MM. All measurements are compatible within experimental errors, showing that the nonlinearity of the sample does not depend on the probed position of the sample. The angle θ between the LC director and the beam polarisation is equal to 18°, and the average value of n_2 is equal to $(-1.09 \pm 0.09) \cdot 10^{-5}$ cm^2·W^{-1}. To evaluate the reproducibility of the Z-scan measurements in polymer-doped samples, we monitor the n_2 value in two nominally identical samples

with the same chemical formulation, for polymer concentrations of 15% and 30% in weight (Figure 2d). For each sample, we measured the nonlinear coefficient in three points to assess its homogeneity. We discard points with recognisable LC alignment defects that generate a remarkable speckle pattern dominating the ballistic transmission. When repeating and comparing these values for nominally identical samples, we find compatible values within the experimental error.

3. Results and discussion

3.1. Nature of the optical nonlinearity

The nature of the collective nonlinearity in dye-doped nematic liquid crystals can be reorientational and/or thermal [30]. In the reorientational case, the optical Kerr effect is due to the molecular reorientation induced by the electric torque that is exerted by the optical electric field on the LC molecules of the sample [13]. In the thermal-optical case, instead, the nonlinear response is caused by temperature and density variations that are driven by the sample absorption, generating what is also defined as a thermal lens [31]. For continuous wave (CW) illumination, the observed nonlinearity can be attributed to refractive index changes caused by a temperature increase. This is supported by the millisecond-scale time response of our system, which is significantly slower than the sub-100 microsecond response typically seen in nonlinear effects driven by density variations [32], as well as by the characterisation provided below.

Focusing on the thermo-optical effect in dye-doped nematic liquid crystals probed with a resonant laser pulse (whose duration is much longer than the acoustic and thermal decay times), absorption determines density and/or temperature variations that drives a thermo-optical effect, to which we can associate the nonlinear refractive index expressed by Equation 1 [32],

$$n2 = (\alpha\tau_R)/(C_v\rho_0)\frac{\partial n}{\partial T} \quad (1)$$

where α is the absorption constant, τ_R is the thermal decay time, ρ_0 is the unperturbed density of the liquid crystal, and C_v is its specific heat at constant volume. It is worth remarking the direct proportionality between the nonlinear response and the absorption coefficient.

The absorbance of PSLCs doped with 1% dye DR1-A at a wavelength of 633 nm is minute, about 0.015, but different from zero. To establish whether this absorption is sufficient to induce a significant variation in temperature and hence the thermo-optical effect, we performed thermal imaging of dye-doped PSLCs with 1% DR1-A and D1-A while illuminated with a red diode laser. Thermal images (acquired with a thermal camera FLIR A400) are shown in Figure 3.

For this characterisation we use a solid-state laser of wavelength $\lambda = 638$ nm, of power $p = 68$ mW and with a beam radius $R \approx 350$ μm. This choice is dictated by the need to reach a laser intensity $I \approx 3.8 \cdot 10^2$ W·cm^{-2}, as high as that which is present in the Z-scan set-up at the focus, but on a larger area, which can be imaged by the thermal camera (100 µm diameter, resolution of the camera). The thermal image for DR1-A presented in Figure 3(a) is acquired with such an intensity and shows a maximum temperature $T = 22.8 \pm 0.5$°C, which is around 1.3°C higher than the environment temperature. When considering the thermal imaging of the dye-doped PSLC with 1% D1-A (Figure 3(b)) instead, it shows a larger temperature variation of around 10°C when exposed to the same laser light intensity. This increase in temperature is associated with a rise in the nonlinear coefficient, as we observe in PSLCs with 20% MM for which the nonlinear refractive index passes from $(-4.2 \pm 0.4) \cdot 10^{-6}$ cm^2 W^{-1} to $(-5.3 \pm 0.5) \cdot 10^{-5}$ cm^2 W^{-1} by changing the doping from 1% dye DR1-A to 1% dye D1-A. This increase is compatible with the absorbance of PSLCs doped with 1%

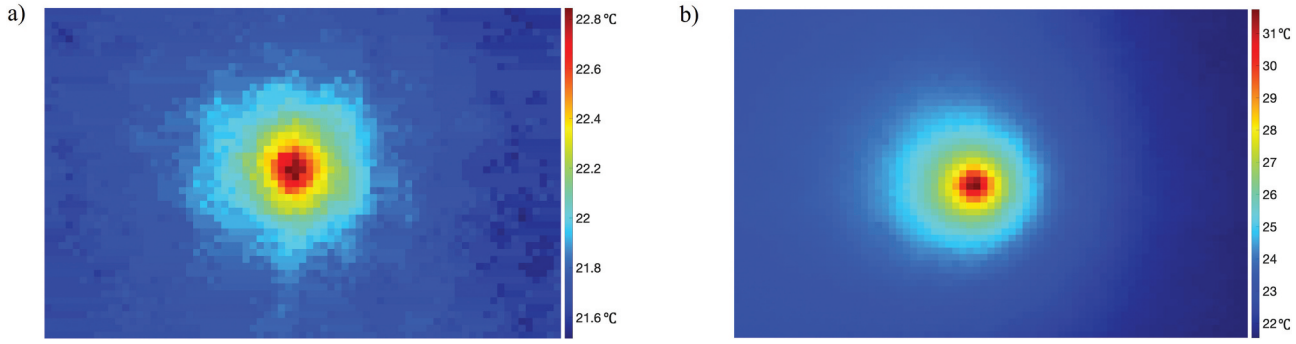

Figure 3. (Colour online) Photo-thermal nature of the third order nonlinearity. Thermal images relating to a dye-doped PSLC with 1% dye DR1-A and 15% monoacrylate monomer MM (panel a) and a dye-doped PSLC with 1% dye D1-A and 20% monoacrylate monomer MM (panel b). These images are acquired with a light intensity which is compatible with those of the optical measurements. The color bars on the right of each image denote the recorded temperatures in Celsius degrees.

dye D1-A that is one order of magnitude higher than that of PSLCs doped with 1% dye DR1-A at 633 nm.

Therefore, the thermal measurements of Figure 3 support the hypothesis of thermo-optical effect, which is consistent with the negative value of the measured nonlinear refractive index [33,34] and the peak to valley distance measured e.g. in Figure 2(b). Indeed, given the values of Δz_{p-v} for the dye-doped PSLCs under examination that are around 3.6, as can be seen in Figure 2(b), this estimate backs up the thermal nature of the measured nonlinear response [28,29].

It is worth noting that the nematic-isotropic transition temperature for the samples doped with DR1-A and those doped with D1-A is $T \approx 37.5$°C and is measured through a hot plate and a polarised optical microscope. While the resolution of the thermal imaging prevents to safely assess that the PSLC with D1-A does not achieve the LC phase transition, the measured nonlinear coefficient for PSLC with D1-A cannot originate from an extraordinary refractive index variation of the liquid crystal 5CB of approximately $\Delta n = 0.12$ that is expected for the nematic-to-isotropic transition [35]. Therefore, we can affirm that the thermo-optical effect that causes the nonlinearity of these samples is not determined by a nematic-to-isotropic transition because of the non-resonant illumination and the very low absorption.

Based on the experimental evidence relating to the thermal measurements and the calculation of the peak-to-valley distances along the z-axis in the Z-scan graph, from now onwards the thermo-optical effect is considered the main cause of the nonlinear response.

3.2. Optimization of the nonlinear response varying the polymer concentration

The optimisation of nonlinearity in dye-doped PSLCs with DR1-A is performed varying the monomer concentration, ranging from 0% to 30%.

All measured n_2 values that are presented hereafter are negative, like those reported in Figure 2(b), and all comments and comparisons are made considering their absolute value.

In order to analyse only the effect of the density of the polymeric structure on the nonlinear refractive index, the dye concentration and the sample thickness are set at 1% and 20 µm, respectively, while the monomer concentration is varied, and all measurements relating to the various concentrations performed with the Z-scan set-up are gathered together in the bar graph of Figure 4(a).

This characterisation highlights one of the main results that we here report for nonlinearity in PSLCs: there is a maximum value of n_2, equal to $(-1.16 \pm 0.09) \cdot 10^{-5}$ $cm^2 \cdot W^{-1}$, at a concentration of the monomer MM of around 10%. This means that the presence of the polymeric structure improves the nonlinear response until the monomer concentration reaches a value for which the polymeric structure hinders the molecular reorientation.

To identify the origin of the growth in the nonlinear response with the polymeric structure, we refer to Equation 1. The nonlinear refractive index is directly proportional to the thermo-optical coefficient $\partial n/\partial T$, which rises up with the presence of the polymeric structure [36] up to when the polymer concentration reaches approximately 10%. For larger monomer concentrations, the decrease in the nonlinear refractive index, instead, can be associated with a decrease of the thermo-optic coefficient of liquid crystals confined in a nanoporous system [37] due to the mechanical constraints imposed by the polymeric structure that affects the order parameter dependence over temperature.

To monitor whether the concentration of the polymeric structure can affect the LC alignment, we studied the order parameter S for the different formulations. From the absorption spectra of the LC sample doped with the

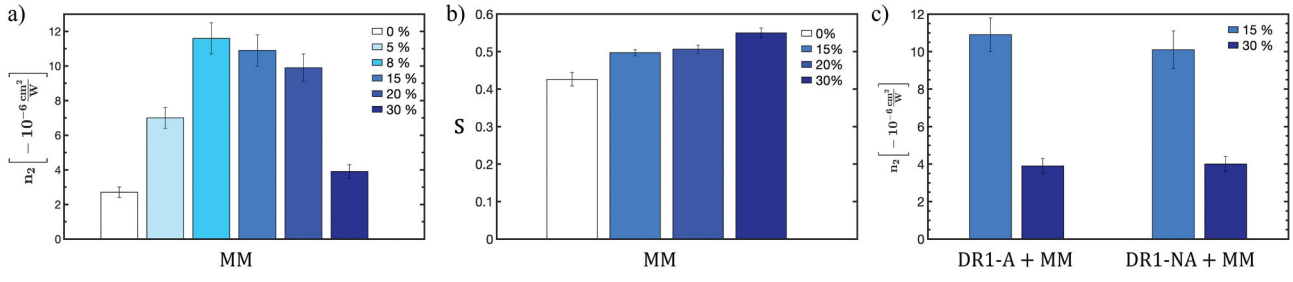

Figure 4. (Colour online) Role of the monomer concentration on the nonlinearity and the order parameter. (a) Dependence of the nonlinear refractive index of a dye-doped PSLC with 1% dye DR1-A on the concentration of the monoacrylate monomer MM. (b) Order parameter of dye-doped PSLCs with 1% dye DR1-A as a function of the concentration of the monoacrylate monomer MM varies. (c) Comparison between the nonlinear refractive indexes of a dye-doped PSLC either with 1% dye DR1-A or 1% dye DR1-NA. In all panels of this figure the legends at the top right of the graphs indicate the monomer concentrations.

dichroic dye molecules, we obtain the order parameter S of the dye-doped PSLC by using Equation 2 [23,38],

$$S = \left(A_{||} - A_{\perp}\right)/\left(A_{||} + 2A_{\perp}\right) \quad (2)$$

where $A_{||}$ and $A_{\perp}$ are the absorbance peaks measured with light beams whose polarizations are parallel and orthogonal to the LC director, respectively. Figure 4(b) presents the dependence of the order parameter on the concentration of the monomer MM. An increase in the order parameter with the concentration is noticed, indicating that polymeric chains made of the mono-acrylate monomer improve the molecular alignment. Such an increase in the order parameter could promote the absorption of the dichroic dye and could thus improve the nonlinear response by the thermo-optical effect although at higher monomer concentration the mechanical constraint dominates over the thermo-optical reorientation. All the nonlinear characterisation reported up to now refer to a PSLC doped with acrylate dyes that ensure a permanent bond with the polymeric structure. To assess the effect of the acrylate nature of the dye on the nonlinear response, we compare the nonlinear refractive index for both acrylate and non-acrylate dyes, that is, DR1-A and DR1-NA, respectively, for a few selected formulations (Figure 4(c)). The nonlinear coefficients are compatible with each other within experimental errors, highlighting that the acrylate nature of the dye seems to not affect the nonlinear response because no absorption variation occurs in the two cases. Moreover, these measurements further support the thermo-optical nature of the nonlinear response, for which we do not expect any influence on the mobility of the dye within the PSLC host.

3.3. Characteristic times of the nonlinear response

To measure the temporal response of nonlinearity, an optical beam shutter is inserted into the Z-scan set-up to modulate laser illumination [39]. We then measured the temporal evolution of the Z-scan curve for the dye-doped PSLC (with 15% MM) and the pure LC with 1% dye DR1-A, taking as the origin of the temporal scale the time when the laser beam passes through the beam shutter with around 50% of its power. Figure 5(a) shows the evolution of the z-scan curve in time from which we retrieve the temporal variation of nonlinear refractive index or the rise time of the nonlinear response (Figure 5(b)) for the PSLC.

The time at which the nonlinear refractive index reaches 90% of its maximum is chosen as the characteristic time of the nonlinear response, and is extracted from an exponential fit performed from the time 0.5 ms. The calculated characteristic time for the PSLC is equal to (1.08 ± 0.03) ms. We repeat the same measurement for the dye-doped LC obtaining a nonlinear response time of (1.69 ± 0.05) ms. The time response is consistent with the thermo-optical nature of the nonlinear effect [12], and is significantly shorter than the characteristic times typical of the optical reorientational effect, which range from tens to hundreds of milliseconds [28]. Moreover, we found out that the polymeric structure not only enhances the nonlinear response but also fastens its dynamics.

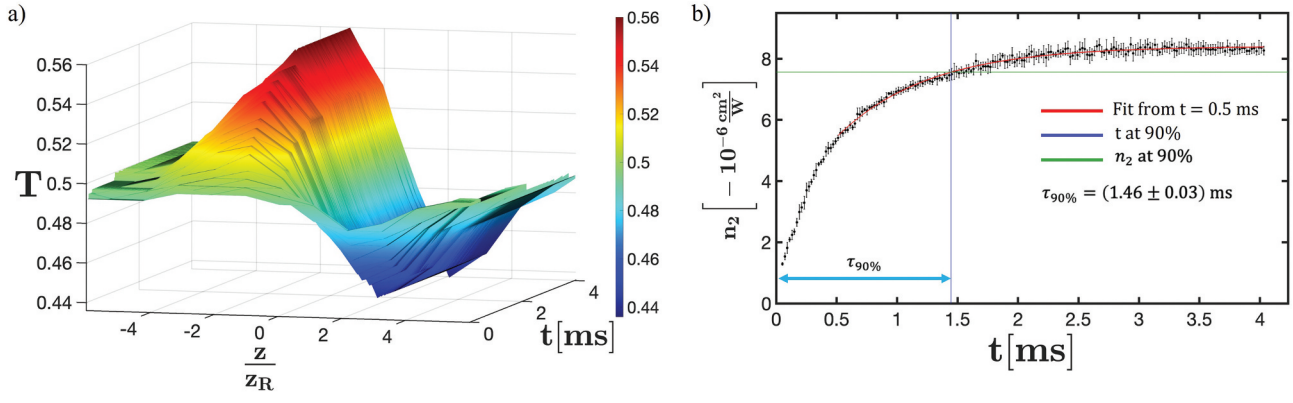

Figure 5. (Colour online) Activation time of the nonlinear response. (a) Temporal evolution of the Z-scan curve. The sample considered here is a dye-doped PSLC with 1% dye DR1-A and 15% monomer MM. The time when the laser beam passes through an optical beam shutter with approximately 50% of its power is taken as the origin of the time axis. (b) Temporal evolution of the nonlinear refractive index relating to the Z-scan curves shown in panel (a). The red line refers to an exponential fit performed with the points acquired at times longer than 0.5 ms. In addition, a violet line corresponding to the time when the nonlinear refractive index reaches 90% of its peak, a green line relating to 90% of the maximum nonlinear coefficient, and the time at which the nonlinear response reaches 90% of its peak, are also shown.

4. Conclusions

In this work, we present the thermo-optical response of dye-doped polymer-stabilised liquid crystals (PSLCs) induced by a low-power continuous-wave laser in pre-resonance conditions. While the nonlinear properties of these materials have been relatively unexplored, we demonstrate their potential for optimising nonlinear effects in dye-doped PSLCs for self-modulation applications with minimal optical losses.

Through Z-scan characterisation and thermal imaging, we confirm that the primary contributor to the nonlinear response, even in pre-resonance conditions, is of thermo-optical origin. This response can be readily tuned by carefully selecting the dye and its absorbance. Furthermore, we show that the nonlinearity and viscosity of the PSLC can be effectively controlled by adjusting the concentration of the polymeric structure, leading to a six-fold improvement in nonlinearity.

Intriguingly, we observe an optimal polymer concentration that maximises the nonlinear response while simultaneously accelerating the nonlinear response time and dynamics. Beyond a certain polymer concentration, the mechanical constraints imposed by the polymer appear to hinder the liquid crystal reorientation. This demonstration on homogeneously aligned films can also be extended to more complex liquid crystal patterns in PSLC [40,41] and open to a spatially modulated thermo-optical response.

This characterisation aims to establish a rigorous basis for a deeper understanding of PSLC nonlinearity, including its dependence on dye contributions, wavelength, and polymeric formulation for new advanced materials for photonics and cryptography.

Acknowledgments

The authors acknowledge Dr. Daniele Martella and Prof. Camilla Parmeggiani for the fruitful discussions on the liquid crystal formulations and Prof. Liana Lucchetti and Dr. Raouf Barboza for the discussions on LC nonlinearity.

Disclosure statement

No potential conflict of interest was reported by the author(s).

Funding

Funded by the European Union [ERC, 3DnanoGiant, n. 101163799]. Views and opinions expressed are however those of the author(s) only and do not necessarily reflect those of the European Union or the European Research Council. Neither the European Union nor the granting authority can be held responsible for them. This work was also supported by the European Union with the funding of the Italian Ministry of University and Research (MUR) within the action Missione 4 Istruzione e ricerca – Componente 2 'Dalla ricerca all'impresa' Investimento 1.1 Fondo per il Programma Nazionale di Ricerca e Progetti di Rilevante Interesse Nazionale (PRIN)" del PNRR – Financed by the European Union – NextGenerationEU under grant PHOTAG [2022T3B4HS, CUP: E53D23005320006]. This work was partially supported by project SERICS (PE00000014) under the MUR National Recovery and Resilience Plan funded by the European Union—NextGenerationEU and co-funded by the European Union—NextGenerationEU, 'Integrated infrastructure initiative in Photonic and Quantum Sciences'—I-PHOQS [IR0000016, ID D2B8D520, CUP B53C22001750006]. FR and SN acknowledge the funding project AFOSR/RTA2 (A.2.e. Information Assurance and Cybersecurity) project 'Highly Secure Nonlinear Optical PUFs' [FA9550–21–1–0039].

References

[1] Deng L, He K, Zhou T, et al. Formation and evolution of far-field diffraction patterns of divergent and convergent gaussian beams passing through self-focusing and self-defocusing media. J Opt A. 2005;7(8):409. doi: 10.1088/1464-4258/7/8/011

[2] Poy G, Hess AJ, Smalyukh II, et al. Chirality- enhanced periodic self-focusing of light in soft birefringent media. Phys Rev Lett. 2020;125(7):077801. doi: 10.1103/PhysRevLett.125.077801

[3] Neufeld O, Cohen O. Optical chirality in nonlinear optics: application to high harmonic generation. Phys Rev Lett. 2018;120(13):133206. doi: 10.1103/PhysRevLett.120.133206

[4] Chen H, Li J, Shang Z, et al. Inverse-designed integrated nonlinear optical switches. Laser Photonics Revs. 2022;16(11):2200254. doi: 10.1002/lpor.202200254

[5] Chai Z, Hu X, Wang F, et al. Ultrafast all-optical switching. Adv Opt Mater. 2017;5(7):1600665. doi: 10.1002/adom.201600665

[6] Nikolopoulos GM. Effects of Kerr nonlinearity in physical unclonable functions. Appl Sci. 2022;12(23):11985. doi: 10.3390/app122311985

[7] Nocentini S, Rührmair U, Barni M, et al. All-optical multilevel physical unclonable functions. Nat Mater. 2014;23(3):369–376. doi: 10.1038/s41563-023-01734-7

[8] Zuo Y, Bi L, Zhao Y, et al. All-optical neural network with nonlinear activation functions. Optica. 2019;6(9):1132–1137. doi: 10.1364/OPTICA.6.001132

[9] Pauwels J, Verschaffelt G, Massar S, et al. Distributed kerr non-linearity in a coherent all-optical fiber-ring reservoir computer. Front Phys. 2019;7:138. doi: 10.3389/fphy.2019.00138

[10] Vermeulen N, Espinosa D, Ball A, et al. Post-2000 nonlinear optical materials and measurements: data tables and best practices. J Phys Photonics. 2023;5(3):035001. doi: 10.1088/2515-7647/ac9e2f

[11] Wang T, Venkatram N, Gosciniak J, et al. Multi-photon absorption and third-order nonlinearity in silicon at mid- infrared wavelengths. Opt Express. 2013;21(26):32192–32198. doi: 10.1364/OE.21.032192

[12] Lin HC, Fuh AYG. Z-scan measurements of optical nonlinearities of dye-doped liquid crystals. J Nonlinear Optic Phys Mat. 2009;18(3):367–400. doi: 10.1142/S0218863509004671
[13] Marrucci L. Mechanisms of giant optical nonlinearity in light-absorbing liquid crystals: a brief primer. Liq Cryst Today. 2002;11(3):6–33. doi: 10.1080/13583140260230264
[14] Khoo IC. Nonlinear optics of liquid crystalline materials. Phys Rep. 2009;471(5–6):221–267. doi: 10.1016/j.physrep.2009.01.001
[15] Dierking I. Polymer network–stabilized liquid crystals. Adv Mater. 2000;12(3):167–181. doi: 10.1002/(SICI)1521-4095(200002)12:3<167::AID-ADMA167>3.0.CO;2-I
[16] Aihara Y, Kinoshita M, Wang J, et al. Polymer stabilization enhances the orientational optical nonlinearity of oligothiophene-doped nematic liquid crystals. Adv Opt Mater. 2013;1(11):787–791. doi: 10.1002/adom.201300326
[17] Wang J, Aihara Y, Kinoshita M, et al. Effect of polymer concentration on self-focusing effect in oligothiophene--doped polymer-stabilized liquid crystals. Opt Mater Expr. 2015;5(3):538–548. doi: 10.1364/OME.5.000538
[18] Wang J, Aihara Y, Kinoshita M, et al. Laser-pointer-induced self-focusing effect in hybrid-aligned dye-doped liquid crystals. Sci Rep. 2015;5(1):9890. doi: 10.1038/srep09890
[19] Jian J, Liu R, Ye Y, et al. Plasmonic-enhanced polymer-stabilized liquid crystals switching for integrated optical attenuation. Adv Opt Mater. 2014;12(19):2400281. doi: 10.1002/adom.202400281
[20] Pöllinger M, Rauschenbeutel A. All-optical signal processing at ultra-low powers in bottle microresonators using the kerr effect. Opt Express. 2010;18(17):17764–17775. doi: 10.1364/OE.18.017764
[21] Zeng H, Martella D, Wasylczyk P, et al. High- resolution 3d direct laser writing for liquid-crystalline elastomer microstructures. Adv Mater. 2014;26:2319–2322. doi: 10.1002/adma.201305008
[22] Martella M, Nocentini S, Nuzhdin D, et al. Photonic microhand with autonomous action. Adv Mater. 2017;29(42):1704047. doi: 10.1002/adma.201704047
[23] Martella D, Nocentini S, Micheletti F, et al. Polarization-dependent deformation in light responsive polymers doped by dichroic dyes. Soft Matter. 2019;15(6):1312–1318. doi: 10.1039/C8SM01954A
[24] Mansare T, Decressain R, Gors C, et al. Phase transformations and dynamics of 4-cyano-4′-pentylbiphenyl (5CB) by nuclear magnetic resonance, analysis differential scanning calorimetry, and wideangle X-ray diffraction analysis. Mol Cryst Liq Cryst. 2002;382(1):97–111. doi: 10.1080/713738756
[25] Creagh LT, Kmetz AR. Mechanism of surface alignment in nematic liquid crystals. Mol Cryst Liq Cryst. 1973;24(1–2):59–68. doi: 10.1080/15421407308083389
[26] Gao Y, Zhang X, Li Y, et al. Saturable absorption and reverse saturable absorption in platinum nanoparticles. Opt Commun. 2005;251(4–6):429–433. doi: 10.1016/j.optcom.2005.03.003
[27] Sheik-Bahae M, Said AA, Wei TH, et al. Sensitive measurement of optical nonlinearities using a single beam. IEEE J Quantum Electron. 1990;26(4):760–769. doi: 10.1109/3.53394
[28] Falconieri M. Thermo-optical effects in Z-scan measurements using high-repetition-rate lasers. J Opt A. 1999;1(6):662. doi: 10.1088/1464-4258/1/6/302
[29] Andrus L, Ben-Yakar A. Thermal lensing effects and nonlinear refractive indices of fluoride crystals induced by high-power ultrafast lasers. Appl Opt. 2020;59(28):8806–8813. doi: 10.1364/AO.400242
[30] Alberucci A, Laudyn UA, Piccardi A, et al. Nonlinear continuous-wave optical propagation in nematic liquid crystals: interplay between reorientational and thermal effects. Phys Rev E. 2017;96(1):012703. doi: 10.1103/PhysRevE.96.012703
[31] Ono H, Takeda K, Fujiwara K. Thermal lens produced in a nematic liquid crystal. Appl Spectros. 1995;49(8):1189–1192. doi: 10.1366/0003702953965083
[32] Khoo IC. Nonlinear optics, active plasmonics and metamaterials with liquid crystals. Prog Quantum Electron. 2014;38(2):77–117. doi: 10.1016/j.pquantelec.2014.03.001
[33] Janossy I, Kosa T. Influence of anthraquinone dyes on optical reorientation of nematic liquid crystals. Opt Lett. 1992;17(17):1183–1185. doi: 10.1364/OL.17.001183
[34] Khoo IC, Li H, Liang Y. Optically induced extraordinarily large negative orientational nonlinearity in dye-doped liquid crystal. IEEE J Quantum Electron. 1993;29(5):1444–1447. doi: 10.1109/3.236160
[35] Cipparrone G, Umeton C, Arabia G, et al. Nonlinear optical effects in polymer dispersed liquid crystals. Mol Cryst Liq Cryst. 1990;179(1):269–275. doi: 10.1080/00268949008055375
[36] McGinty C, Reich R, Clark H, et al. Enhancing the thermo-optical response of nematic liquid crystal with a polymer network. J Appl Phys. 2020;127(2):024504. doi: 10.1063/1.5122987
[37] Batalioto F, Evangelista LR, Barbero G. Effect of the incomplete interaction on the nematic–isotropic transition at the nematic–wall interface. Phys Lett A. 2004;324(2–3):198–202. doi: 10.1016/j.physleta.2004.02.070
[38] Kondo M, Sugimoto M, Yamada M, et al. Effect of concentration of photoactive chromophores on photomechanical properties of crosslinked azobenzene liquid-crystalline polymers. J Mater Chem. 2010;20(1):117–122. doi: 10.1039/B917342K
[39] Falconieri M, Salvetti G. Simultaneous measurement of pure-optical and thermo- optical nonlinearities induced by high-repetition-rate, femtosecond laser pulses: application to cs2. Appl Phys B. 1999;69(2):133–136. doi: 10.1007/s003400050785
[40] Wu JB, Wu SB, Cao HM, et al. Electrically tunable microlens array enabled by polymer-stabilized smectic hierarchical architectures. Adv Opt Mater. 2022;10(20):2201015. doi: 10.1002/adom.202201015
[41] Wu SB, Wu JB, Cao HM, et al. Topological defect guided order evolution across the nematic-smectic phase transition. Phys Rev Lett. 2023;130(7):078101. doi: 10.1103/PhysRevLett.130.078101